Inorg. Chem. **2009**, *48*, 2670−2676

Ground- and Excited-State Dynamics of Aluminum and Gallium Corroles

Dorota Kowalska,[†] Xia Liu,[†] Umakanta Tripathy,[†] Atif Mahammed,[‡] Zeev Gross,*[,‡] Satoshi Hirayama,[†] and Ronald P. Steer*[,†]

Department of Chemistry, University of Saskatchewan, 110 Science Place, Saskatoon, SK, Canada S7N 5C9, and Schulich Faculty of Chemistry, Technion − Israel Institute of Technology, Haifa 32000, Israel

Received January 12, 2009

The steady-state absorption and emission spectra and the temporal fluorescence decay profiles of two metallocorroles, Al(tpfc)(py)$_n$ and Ga(tpfc)(py)$_n$ (n = 1,2), have been measured in a noncoordinating solvent, benzene, in a coordinating solvent, pyridine, and in mixed benzene−pyridine solutions. The ground-state spectra reveal that an equilibrium between the pentacoordinate corrole (n = 1) and the hexacoordinate corrole (n = 2) is established in the mixed benzene−pyridine solutions. The ground-state equilibrium constants are 135 M^{-1} and 1.0 M^{-1} at 295 K for the Al and Ga species, respectively. The excited-state radiative and nonradiative decay constants of the pentacoordinate and the hexacoordinate species have been obtained from measurements of the fluorescence quantum yields and monoexponential fluorescence decay times in pure benzene and pure pyridine. Temporal fluorescence decays of the gallium system in a mixed benzene−pyridine solution are biexponential due to dissociation of the hexacoordinate species in the excited state leading to the establishment of a dissociation−association equilibrium. The rate constants for the pyridine association and dissociation processes for the gallium corrole in the excited state have been measured, $k_a^* = 2.3 \times 10^8$ M^{-1} s^{-1} and $k_d^* = 2.9 \times 10^8$ s^{-1}, respectively, leading to a value for the excited-state association equilibrium constant of $K_a^* = 0.78$ M^{-1}.

Introduction

Research interest in the corroles, porphyrin-like tetrapyrrolic macrocycles, has been widespread since the first practical methods of triarylcorrole synthesis were disclosed in 1999.[1−8] One of the four bridging methine groups in porphyrins is absent in the corroles, so that the corrole macrocycle in metal-chelated derivatives belongs to the C_{2v} point group (cf. D_{4h} for the metalloporphyrins). The corrole macrocycle thus possesses a smaller cavity for metal coordination than that of the porphyrins and accommodates trivalent group 13 metals (cf. zinc(II) and magnesium(II) porphyrins) such as aluminum(III) and gallium(III) that can bind up to two additional axial ligands.[4−6]

Recently, the emphasis in corrole research has been devoted to understanding the unique electronic structures and chemical properties of their transition metal complexes and to using them as catalysts for a variety of processes.[9−14] Metal-free (commonly called free-base) corroles and their chelates with nontransition metal ions have received less

* To whom correspondence should be addressed. Phone: (306) 966-4667 (R.P.S.), (972) 4829-3954 (Z.G.). Fax: (306) 966-4730 (R.P.S.), (972) 4829-5703 (Z.G.). E-mail: ron.steer@usask.ca (R.P.S.), chr10zg@tx.technion.ac.il (Z.G.).
† University of Saskatchewan.
‡ Technion − Israel Institute of Technology.

(1) Gross, Z.; Galili, N.; Saltsman, I. *Angew. Chem., Int. Ed.* **1999**, *38*, 1427.
(2) Paolesse, R.; Jaquinod, L.; Nurco, D. J.; Mini, S.; Sagone, F.; Boschi, T.; Smith, K. M. *Chem. Commun.* **1999**, 1307.
(3) Erlen, C.; Will, S.; Kadish, K. M. In *The Porphyrin Handbook*; Kadish, K. M.; Smith, K. M.; Guilard, R., Eds.; Academic Press: New York, 2000; Vol. 2, pp 233−300.
(4) Bendix, J.; Dmochowski, I. J.; Gray, H. B.; Mahammed, A.; Simkhovich, L.; Gross, Z. *Angew. Chem., Int. Ed.* **2000**, *39*, 4048.
(5) Mahammed, A.; Gross, Z. *J. Inorg. Biochem.* **2002**, *88*, 305.
(6) Sorasaenee, K.; Taqavi, P.; Heling, L. M.; Gray, H. B.; Tkachenko, E.; Mahammed, A.; Gross, Z. *J. Porphyrins Phthalocyanines* **2007**, *11*, 189.
(7) Nardis, S.; Monti, D.; Paolesse, R. *Min-Rev. Org. Chem.* **2005**, *2*, 355.
(8) Gross, Z. *J. Biol. Inorg. Chem.* **2001**, *6*, 733.
(9) Ye, S.; Tuttle, T.; Bill, E.; Simkhovich, L.; Gross, Z.; Thiel, W.; Neese, F. *Chem.−Eur. J.* **2008**, *14*, 10839.
(10) Simkhovich, L.; Mahammed, A.; Goldberg, I.; Gross, Z. *Chem.−Eur. J.* **2001**, *7*, 1041.
(11) Mahammed, A.; Gross, Z. *J. Am. Chem. Soc.* **2005**, *127*, 2883.
(12) Gross, Z.; Gray, H. B. *Adv. Synth. Catal.* **2004**, *346*, 165.
(13) Mahammed, A.; Gross, Z. *Angew. Chem., Int. Ed.* **2006**, *45*, 6544.
(14) Haber, A.; Mahammed, A.; Fuhrman, B.; Volkova, N.; Coleman, R.; Hayek, T.; Aviram, M.; Gross, Z. *Angew. Chem., Int. Ed.* **2008**, *47*, 7896.

10.1021/ic900056n CCC: $40.75
Published on Web 02/10/2009

Scheme 1

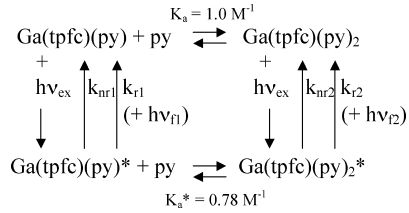

attention, despite the fact that some early studies of their spectroscopic and photophysical properties revealed that they would be attractive potential alternatives to the porphyrins[15,16] used in dye-sensitized photovoltaic cells and photodynamic therapy and proposed for use in photon-actuated molecular logic devices. These properties include large quantum yields of S_1-S_0 fluorescence,[4,5] dual S_2-S_0 and S_1-S_0 fluorescence,[17] large quantum yields of singlet molecular oxygen in oxygenated solutions,[18] and facile synthetic access to water-soluble derivatives.[19,20]

The effects of substituents and their position on the photophysical properties of free-base corroles and of some corrole-containing dyads have been reported recently,[18,21,22] but similar information about their metallated derivatives is sparse. In particular, the effects of noncovalent axial ligand binding on the spectroscopic and photophysical properties of the metallocorroles have not yet been thoroughly investigated, even though such insight may be very important given the increasing interest in applying corroles in biological media.[14,16] We have collaborated to fill this information gap by examining the coordination dynamics of two metallocorroles, Al(tpfc)(py)$_n$ and Ga(tpfc)(py)$_n$ ($n = 1, 2$) (cf. Scheme 1), in both the ground and excited states. The combination of approaches adopted in this investigation has resulted in the first measurements of ligand association−dissociation reaction rate constants of metallocorroles in their electronic excited states.

Results and Discussion

Al(tpfc)(py)$_n$ and Ga(tpfc)(py)$_n$ are both five-coordinate ($n = 1$) when dissolved in noncoordinating solvents such as benzene and toluene, used here.[17] A ground-state equilibrium between the five-coordinate and the six-coordinate ($n = 2$) species is established when pyridine, py, is added to such a solution, namely,

$$\mathrm{M(tpfc)(py) + py \rightleftarrows M(tpfc)(py)_2} \qquad (1)$$

whereas only the fully six-coordinate species is found in pure pyridine. The effects on the absorption and fluorescence emission spectra of adding incremental amounts of pyridine to a benzene solution of Ga(tpfc)(py)$_n$ are illustrated in and Figure 1b and d. Figure 1a and c show the distinct shift in the transition energies of the absorption and emission spectra of Al(tpfc)(py)$_n$ when pyridine is substituted for benzene as the solvent. In both corroles, the six-coordinate species absorbs and emits further to the red than the five-coordinate one, leading to clear isosbestic points in the absorption spectra near 602, 578, 572, and 566 nm in the Q bands and near 400 and 425 nm in the Soret bands for Ga(tpfc)(py)$_n$. Isoemissive points appear near 608, 643, and 665 nm in its S_1 (Q-band) fluorescence spectra. For Al(tpfc)(py)$_n$, the corresponding isosbestic points are located at very similar wavelengths, 602 and 426 nm, whereas the isoemissive points are somewhat further red-shifted at 612, 647, and 669 nm.

The metalloporphyrins exhibit bathochromic shifts in their UV−visible spectra that are linear functions of the Lorenz−Lorentz polarizability function of the solvent, $f_1 = (n^2 - 1)/(n^2 + 2)$, indicating that dispersive solute−solvent interactions dominate their solvatochromism.[23] The refractive indices, n, of pyridine and benzene are almost identical, leading to values of f_1 that differ only in the third significant digit. The corroles and their metalloporphyrin analogs are expected to exhibit similar solvatochromic behavior in solution, so any solvatochromically induced shifts in their absorption spectra will be essentially independent of the composition of the benzene−pyridine mixtures. Thus, the red shifts in the absorption and emission spectra observed when pyridine replaces benzene as a solvent must be due exclusively to the formation of the six-coordinate species. The five-coordinate species is clearly stabilized by the second axial pyridine ligand. Using the Q- and Soret-band spectral shifts as a measure of the difference between the energies of the ground and excited electronic states, we note that stabilization produced by adding a second pyridine ligand is smaller for the gallium corrole than for the aluminum corrole and is smaller in the S_2 states of both molecules than in their S_1 states.

Quantitative analyses of the absorption spectra as a function of pyridine concentration yield values of the equilibrium constants for the ground-state association reactions, eq 1 above. Under conditions where [py] ≫ [M(tpfc)(py)$_1$], plots of $(\Delta A)^{-1}$ versus $[\mathrm{py}]^{-1}$ are expected to be linear,[24,25] as shown in Figure 2 for Ga(tpfc)(py)$_n$ in benzene. Here, ΔA is the change in absorbance of the Q-band absorption spectrum of Ga(tpfc)(py)$_n$ in benzene with added pyridine (in Figure 2 for the Ga(tpfc)(py)$_2$ band maximum at 612 nm), and [py] is the molar concentration of pyridine. The ratio of the intercept to slope of such plots equals the value of the ground-state association constant, K_a, which equals 1.0 M^{-1} for Ga(tpfc)(py)$_n$ at 295 K. The six-coordinate aluminum corrole is considerably more stable

(15) Tripathy, U.; Steer, R. P. *J. Porphyrins Phthalocyanines* **2007**, *11*, 228.
(16) Aviv, I.; Gross, Z. *Chem. Commun.* **2007**, 1987.
(17) Liu, X.; Tripathy, U.; Mahammed, A.; Gross, Z.; Steer, R. P. *Chem. Phys. Lett.* **2008**, *459*, 113.
(18) Ventura, B.; Esposti, A. D.; Koszarna, B.; Gryko, D. T.; Flamigni, L. *New J. Chem.* **2005**, *29*, 1557.
(19) Aviezer, D.; Cotton, S.; David, M.; Segev, A.; Khaslev, N.; Galili, N.; Gross, Z.; Yayon, A. *Cancer Res.* **2000**, *60*, 2973.
(20) Saltman, I.; Mahammed, A.; Goldberg, I.; Tkachenko, E.; Botoshansky, M.; Gross, Z. *J. Am. Chem. Soc.* **2002**, *12*, 4–7411.
(21) Paolesse, R.; Sagnore, F.; Macagnano, A.; Boschi, T.; Prodi, L.; Montalli, M.; Zacchereni, N.; Bolletta, F.; Smith, K. M. *J. Porphyrins Phthalocyanines* **1999**, *3*, 364.
(22) Ding, T.; Aleman, E. A.; Modarelli, D. A.; Ziegler, C. J. *J. Phys. Chem. A* **2005**, *109*, 7411.
(23) Liu, X.; Tripathy, U.; Bhosale, S. V.; Langford, S. J.; Steer, R. P. *J. Phys. Chem. A* **2008**, *112*, 8986.
(24) Benesi, H. A.; Hildebrand, J. H. *J. Am. Chem. Soc.* **1949**, *71*, 2703.
(25) Novokov, E.; Boens, N. *J. Phys. Chem. A* **2007**, *111*, 6054.

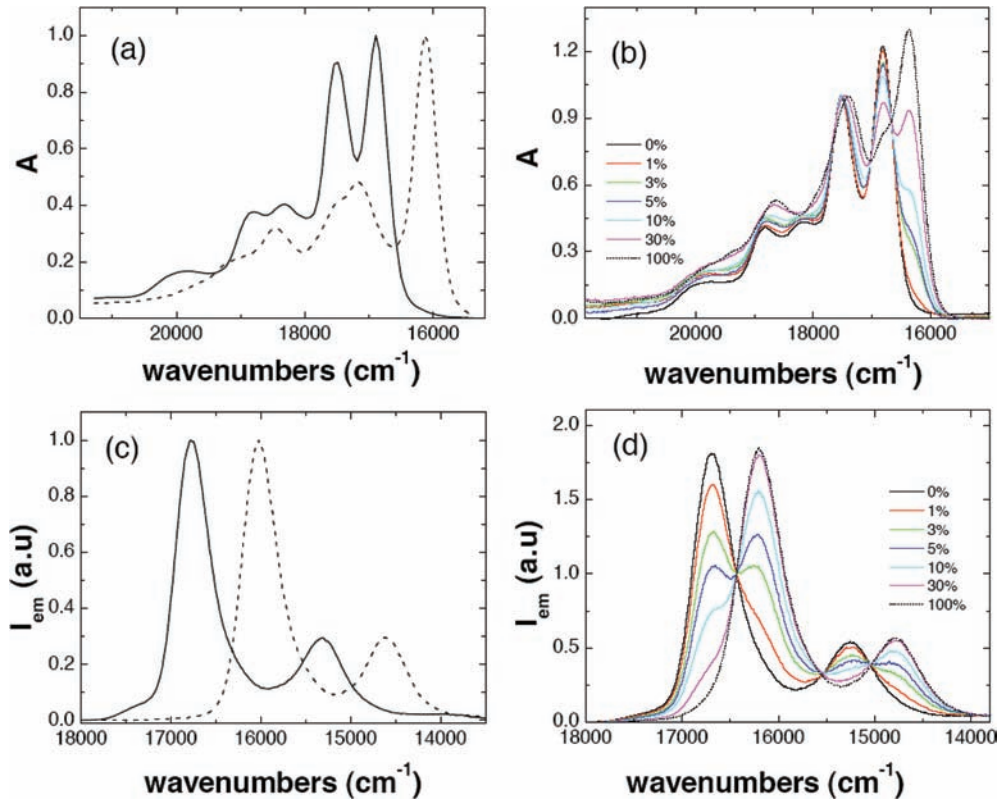

Figure 1. Absorption (a) and emission (c) spectra of Al(tpfc)(py)$_n$ in benzene and pyridine and absorption (b) and emission (d) spectra of Ga(tpfc)(py)$_n$ in benzene as a function of added pyridine (increasing, as shown; 0, 1, 3, 5, 10, 30, and 100% by volume for d and 0, 2, 4, 6, 10, and 15% by volume for b).

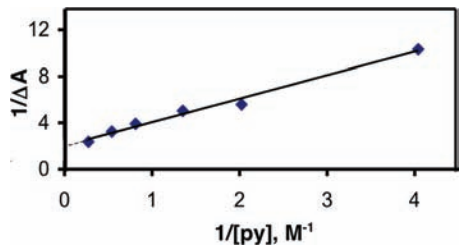

Figure 2. Benesi−Hildebrand plot of $(\Delta A)^{-1}$ at 612 nm versus $[py]^{-1}$ for Ga(tpfc)(py)$_n$ in benzene at room temperature.

than its gallium counterpart; that is, aluminum(III) acts as a significantly stronger Lewis acid than gallium(III) in these corroles. The corresponding value of K_a is 135 M^{-1} for the Al(tpfc)(py)$_n$ system in benzene at 295 K.

Time-correlated single-photon counting measurements of the S_1 fluorescence lifetimes of the two metallocorroles in deoxygenated solutions of pure benzene and pure pyridine yielded the data presented in Figure 3a and Table 1. The temporal fluorescence decay profiles of each compound in both pure solvents are well-modeled by single exponential functions ($1.00 < \chi^2 < 1.10$) with lifetimes that are similar in magnitude, but nevertheless significantly different, for the five- and the six-coordinate species. The quantum yields of $S_1 \rightarrow S_0$ fluorescence of these corroles in a variety of media have been measured previously.[5] The rate constants of the radiative decay and the sums of the rate constants of the nonradiative decay processes of these five- and six-coordinate species in their S_1 states may thus be calculated from $k_r = \phi_f/\tau$ and $\Sigma k_{nr} = (1 - \phi_f)/\tau$. The data are compiled in Table 1.

The fluorescence lifetimes of the gallium corroles are substantially shorter that those of the corresponding aluminum compounds, due almost exclusively to their larger S_1 radiationless decay constants. This difference in the radiationless decay rates of the two metallocorroles is consistent with a faster rate of S_1-T_1 intersystem crossing in the gallium compound due to its enhanced heavy-atom-induced spin−orbit coupling. Similar heavy-atom effects have been reported previously in the S_1-T_1 decay rates of the d^0 and d^{10} metalloporphyrins.[26] Curiously, however, again due primarily to differences in their radiationless decay rates, the S_1 lifetime of the six-coordinate aluminum corrole (6.60 ns in pyridine) is somewhat shorter that that of the five-coordinate species (7.34 ns in benzene), whereas the lifetime of the S_1 state of the six-coordinate gallium compound (3.45 ns in pyridine) is slightly longer that its five-coordinate counterpart (3.04 ns in benzene).

In the Al(tpfc)(py)$_n$ system, the large value of the ground-state association constant made it impossible to excite significant amounts of the five-coordinate species at pyridine concentrations where the excited-state association reaction rates and the excited-state decay rates were comparable and the effect of added pyridine could be observed in the fluorescence decay. However, this was not the case for the Ga(tpfc)(py)$_n$ system in which $K_a = 1.0$ M^{-1}. Temporal S_1 fluorescence decay profiles of Ga(tpfc)(py)$_n$ were measured as a function of the concentration of pyridine added to benzene solutions of the (initially) five-coordinate corroles,

(26) Harriman, A. *J. Chem. Soc., Faraday Trans. 2* **1981**, *77*, 1281.

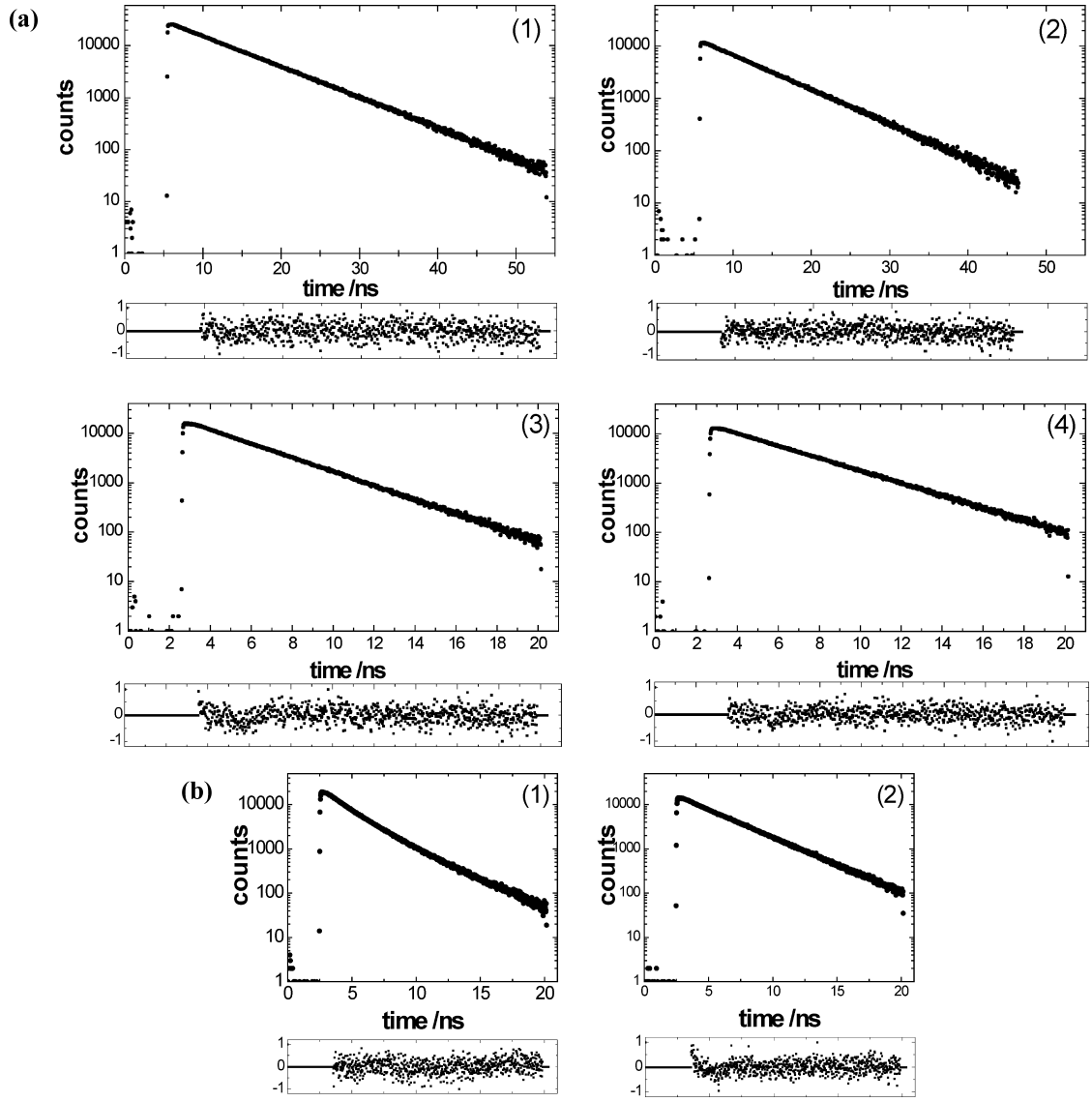

Figure 3. (a) S_1-fluorescence decays for Al(tpfc)(py)$_n$ in (1) benzene, $\tau = 7.34$ ns, $\chi^2 = 1.07$, and (2) in pyridine, $\tau = 6.60$ ns, $\chi^2 = 1.08$, and Ga(tpfc)(py)$_n$ in (3) benzene, $\tau = 3.04$ ns, $\chi^2 = 1.10$, and (4) in pyridine, $\tau = 3.45$ ns, $\chi^2 = 1.10$, at room temperature. (b) S_1-fluorescence decays for Ga(tpfc)(py)$_n$ in (1) benzene + 3% pyridine, $\tau_1 = 3.15$ ns, $\tau_2 = 1.55$ ns, $\chi^2 = 1.08$, and (2) benzene + 30% pyridine, $\tau_1 = 3.41$ ns, $\tau_2 = 0.68$ ns, $\chi^2 = 1.10$, at room temperature.

Table 1. Photophysical Data for the S_1 States of Al(tpfc)(py)$_n$ and Ga(tpfc)(py)$_n$ in Deoxygenated Benzene and Pyridine Solutions at Room Temperature

solvent	λ_{ex}, nm	λ_{em}, nm	τ, ns	ϕ_f[a]	k_r, $\times 10^8$ s^{-1}	Σk_{nr}, $\times 10^7$ s^{-1}
			M = Al			
benzene ($n = 1$)	400	596	7.34	0.76	1.03	3.27
pyridine ($n = 2$)	400	624	6.60	0.76	1.15	3.64
			M = Ga			
benzene ($n = 1$)	400	599	3.04	0.37	1.22	20.7
pyridine ($n = 2$)	400	617	3.45	0.47	1.36	15.4

[a] Data from ref 5; solvent for $n = 1$ is toluene with λ_{ex} in the Q band.

with results that are shown in Figure 3b. Iterative convolution of the instrument response function with trial fluorescence decay functions revealed that the fluorescence profiles of the corroles in the benzene−pyridine mixtures are all biexponential, that is, of the form $I(t) = a_1 \exp(-t/\tau_1) + a_2 \exp(-t/\tau_2)$. The fraction of the total fluorescence intensity associated with each component of the double exponential was obtained from the fitting parameters using the expression $F_i = a_i\tau_i/\Sigma a_i\tau_i$. Data were obtained as a function of solution composition and for several excitation and emission wavelengths; they are collected in Table 2. No evidence of a fluorescent species with a measurable rise time was obtained in these systems.

Note that the benzene−pyridine solutions were excited exclusively at or near the two isosbestic points in the Soret bands of the corroles, resulting in the initial population of the S_2 states of the five- or the six-coordinate species or of both. Previous work[17] has demonstrated that the lifetimes of these initially excited S_2 states lie in the 200−300 fs region for both the aluminum and gallium corroles, that their quantum yields of S_2-S_1 internal conversion are both ca. 0.8, and that the S_1 emission spectra obtained for each corrole are identical when exciting in either the Soret or the Q absorption bands. Thus, the kinetic phenomena observed here

Table 2. Photophysical Data for the S_1 State of Ga(tpfc)(py)$_n$ (n = 1, 2) in Deoxygenated Benzene−Pyridine Mixtures at Room Temperature

solvent	[py], M	λ_{ex}, nm	λ_{em}, nm	τ_1, ns	τ_2, ns	F_1[a]	x_1[b]
benzene	0	400	605	3.04		1	1
+1% py	0.124	400	605	2.98	1.74	0.88	0.99
+3% py	0.372	400	605	3.15	1.55	0.57	0.97
+5% py	0.621	400	605	3.24	1.49	0.52	0.95
		400	620	3.29	1.34	0.94	
		400	660	3.30	1.42	0.91	
		400	680	3.30	1.42	0.96	
		425	605	3.24	1.50	0.53	
		425	620	3.31	1.38	0.93	
+10% py	1.24	400	620	3.41	1.09	0.94	0.89
+30% py	3.72	400	620	3.41	0.68	0.98	0.68
pyridine		400	620	3.45		1	0

[a] Fraction of emission intensity due to component 1; $F_2 = 1 - F_1$. [b] Mole fraction of Ga(tpfc)(py)$_1$; mole fraction of Ga(tpfc)(py)$_2$ is $x_2 = 1 - x_1$.

on a nanosecond time scale are clearly associated with processes occurring in the vibrationally relaxed S_1 states of the molecular species present in solution.

The corrole concentrations were sufficiently dilute ($c < 10^{-5}$ M) that aggregation of the solute was not significant; differences in the photophysical behavior of the solute as a function of solution composition were therefore attributed solely to the effects of the ground-state equilibrium represented by eq 1 and by the corresponding excited-state reactions leading to equilibrium in which the ligated corroles are radiating from their S_1 excited states (cf. Scheme 1). Any effects due to ligand dissociation of the five-coordinate species in the excited state were ruled out because the temporal fluorescence decay profile of the five-coordinate species excited in pure benzene is single exponential; that is, there is no evidence of emission from an excited M(tpfc)(py)$_n$, $n = 0$, species.

Note the following from the data for the Ga(tpfc)(py)$_n$ system in Tables 1 and 2: (i) The measured "lifetime" of the longer-lived fluorescent component in the pyridine−benzene mixtures is independent of observation wavelength and, within experimental error, moves monotonically with increasing pyridine concentration from the lifetime of excited Ga(tpfc)(py) in benzene (3.04 ± 0.05 ns) to the lifetime of excited Ga(tpfc)(py)$_2$ in pyridine (3.45 ± 0.05 ns). (ii) The lifetime of the shorter-lived component of the fluorescence decreases monotonically with increasing pyridine concentration but is (within experimental error) independent of observation wavelength, suggesting perhaps that it is associated with the kinetics of the ligand association−dissociation reaction in the excited state (vide infra). (iii) The fraction of the total emission due to the long-lived component decreases with increasing pyridine content when observed at the isoemissive wavelength and is much larger (approaching 1) when observing emission at the band maxima of the emission spectrum of the six-coordinate species. The fraction of the total emission associated with the short-lived component of the fluorescence decay varies in the opposite sense and approaches zero at the largest pyridine concentrations when observing in the emission bands of the six-coordinate species. (iv) The values of τ_i and F_i are the same for excitation at the two isosbestic wavelengths within the Soret-band system.

Two absorbing corrole species are present at equilibrium in the benzene−pyridine mixtures, and the relative amounts of each change with changing solution composition. The mole fractions, x_1 and x_2, of the five- and six-coordinate gallium corroles calculated from the measured ground-state association constant are given in Table 2. If the species-weighted average "lifetimes" of the S_1 states of Ga(tpfc)(py)$_1$ and Ga(tpfc)(py)$_2$ are calculated using the same mole fractions of the two species that exist in the ground state (i.e., from $\tau = \Sigma x_i \tau_i$ using the data of Table 2), the resulting weighted lifetimes are slightly longer than the observed ones. That is, such a calculation systematically overestimates the contribution from the longer-lived six-coordinate species. This suggests that the equilibrium constant for the association−dissociation reaction in the excited state of the Ga(tpfc)(py)$_n$ system should be somewhat smaller, but not much smaller, than the ground-state value of $K_a = 1.0\ M^{-1}$. Moreover, excitation of the system at equilibrium in the ground state will produce an initially nonequilibrium distribution of excited state five- and six-coordinate species whose approach to equilibrium results in the observed biexponential fluorescence decay on a time scale similar to those of the lifetimes of the excited species. The best fit for the excited-state association equilibrium constant is found by independent calculation to be $K_a^* = 0.78 \pm 0.07\ M^{-1}$ (vide infra).

Values of the rate constants for the association reaction of the five-coordinate species with pyridine and the dissociation of the six-coordinate species in the excited state were determined from a kinetic model baed on Scheme 1. We define k_a^* and k_d^* as the rate constants for the forward (association) and reverse (dissociation) processes in the excited state, eq 2:

$$\text{M(tpfc)(py)}^* + \text{py} \rightleftarrows \text{M(tpfc)(py)}_2^* \qquad (2)$$

Thus, $K_a^* = k_a^*/k_d^*$, and $k_{PC} = (1/\tau_1)_{PC} = 3.29 \times 10^8\ s^{-1}$ is the overall (radiative plus nonradiative) first-order decay constant for the pentacoordinate species in benzene, whereas $k_{HC} = (1/\tau_1)_{HC} = 2.90 \times 10^8\ s^{-1}$ is the overall first-order decay constant for the hexacoordinate species in pyridine. The model in Scheme 1 is very similar to that used to describe the excited-state kinetics of radiative exciplexes, except that in the present system, the two radiative species may be excited directly from their ground states due to the operation of the ground-state association equilibrium. The well-established exciplex kinetics analysis of Hui and Ware[27,28] was therefore applied to this system, using the data in Table 2 to construct simultaneous equations from which the two unknown rate constants are calculated (cf. Supporting Information). Iterative fitting of these data results in values of $k_a^* = (2.2 \pm 0.2) \times 10^8\ M^{-1}\ s^{-1}$, $k_d^* = (2.9 \pm 0.1) \times 10^8\ s^{-1}$, and $K_a^* = 0.78 \pm 0.07\ M^{-1}$ for the Ga(tpfc)(py)$_n$ system. Note that the value of $K_a^* = 0.78\ M^{-1}$ is slightly smaller than the value of $K_a = 1.0\ M^{-1}$, as predicted by the qualitative argument presented above. Note also that the value of $k_a^* = (2.2 \pm 0.2) \times 10^8\ M^{-1}\ s^{-1}$ is considerably smaller (by a factor of about 40−50) than the diffusion-limited value of $1.0 \times 10^{10}\ M^{-1}\ s^{-1}$ in benzene at 295 K.

(27) Hui, M.-H.; Ware, W. R. *J. Am. Chem. Soc.* **1976**, *98*, 4712.
(28) Hui, M.-H.; Ware, W. R. *J. Am. Chem. Soc.* **1976**, *98*, 4718.

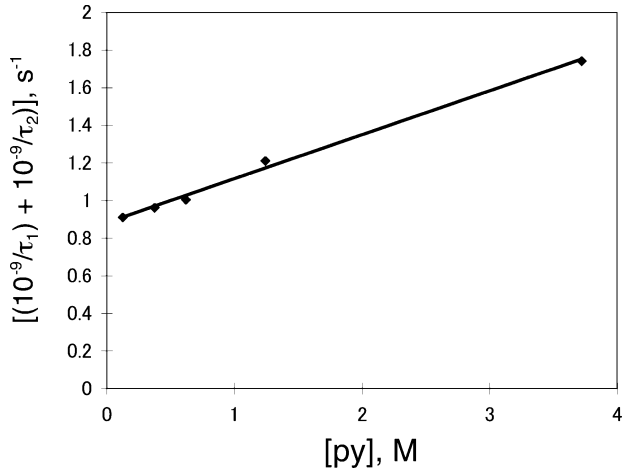

Figure 4. Plot showing $-(\lambda_1 + \lambda_2) = (\tau_1)^{-1} + (\tau_2)^{-1}$ versus [py] for Ga(tpfc)(py)$_n$ in benzene at room temperature. The slope is 2.3×10^8 M^{-1} s^{-1} = k_a*.

This is entirely reasonable, given that productive coordination of the second ligand can only occur from the unligated side of the five-coordinate species, and then only when the N atom of the pyridine is appropriately oriented toward the macrocycle.

The short-lived component of the measured biexponential decays in the benzene−pyridine mixtures has a measured lifetime that is independent of the observation wavelength and that decreases with increasing pyridine concentration. In addition, the fraction of the emission of the shorter-lived component is considerably smaller when observing at wavelengths where the six-coordinate species emits. This suggests that this short-lived component is associated with emission from the excited five-coordinate species that is being removed by the pseudo-first-order ligand association process described in eq 2. In the kinetic model employed, $-(\lambda_1 + \lambda_2) = (1/\tau_1 + 1/\tau_2)$ is equal to the sum of the first-order and pseudo-first-order rate constants of the parallel processes by which the two excited species decay, that is, $(1/\tau_1 + 1/\tau_2) = k_{HC} + k_d* + k_{PC} + k_a*[py]$. The plot of $(1/\tau_1 + 1/\tau_2)$ versus [py] is shown in Figure 4. A good linear relationship is obtained, and the slope yields a value of $k_a* = (2.3 \pm 0.1) \times 10^8$ M^{-1} s^{-1}, which is in excellent agreement with the value of $k_a* = (2.2 \pm 0.2) \times 10^8$ M^{-1} s^{-1} calculated from the best fit to the kinetic model described above (cf. Supporting Information).

Conclusions

The steady-state absorption and emission spectra and the temporal fluorescence decay profiles of two metallocorroles, Al(tpfc)(py)$_n$ and Ga(tpfc)(py)$_n$ (n = 1, 2), have been measured in a noncoordinating solvent, benzene, in a coordinating solvent, pyridine, and in mixed benzene−pyridine solutions. The ground-state spectra reveal that an equilibrium between the pentacoordinate corrole (n = 1) and the hexacoordinate corrole (n = 2) is established in the mixed benzene−pyridine solutions. The ground-state equilibrium constants are 135 M^{-1} and 1.0 M^{-1} at 295 K for the Al and Ga species, respectively. The excited-state radiative and nonradiative decay constants of the pentacoordinate and the hexacoordinate species have been obtained from measurements of the fluorescence quantum yields and fluorescence decay times in pure benzene and pure pyridine, respectively. The steady-state and time-resolved measurements all suggest that coordination of the metal by a second pyridine molecule stabilizes the corrole, with the lowest excited singlet state (present work) stabilized more than the second excited singlet (past work[17]) state and the aluminum corrole stabilized more than the gallium species.

Temporal fluorescence decays of the gallium system in a mixed benzene−pyridine solution are biexponential due to dissociation of the hexacoordinate species in the excited state, leading to establishment of an excited-state dissociation−association equilibrium. The rate constants for the pyridine association and dissociation processes for the gallium corrole in the excited state have been extracted using a kinetic scheme similar to that employed for excimer photophysics; the values are $k_a* = 2.3 \times 10^8$ M^{-1} s^{-1} and $k_d* = 2.9 \times 10^8$ s^{-1}, leading to a value for the excited-state association equilibrium constant of $K_a* = 0.78$ M^{-1}. To our knowledge, these are the first rate constants to be measured for excited-state ligand association−dissociation reactions in metallocorrole systems. We expect that the information and methodologies provided in this manuscript will be very useful in the design of tailor-made corroles that can be used in various applications.

Experimental Section

The Al and Ga corroles were synthesized as reported previously.[4,5] All experiments were carried out in benzene, pyridine, or mixed benzene−pyridine solutions at room temperature. Solvents (Aldrich) were of the highest available purity and exhibited negligible fluorescence at the excitation wavelengths employed. Deoxygenation was effected by purging the solutions with dry, O_2-free nitrogen. No significant photodegradation of the corroles was observed due to brief exposure to room light, to the narrow spectral bandwidths of the Xe arc lamps in the steady-state spectrometers, or to picosecond pulsed laser light during fluorescence lifetime measurements.

Absorption spectra were recorded on a Varian (Cary) 500 UV−visible spectrophotometer. Steady-state fluorescence measurements were performed using a Photon Technology International QuantaMaster spectrofluorometer fitted with double monochromators on both the excitation and emission sides and a calibrated photodiode for correction of the excitation spectra. The emission spectra were corrected for detector sensitivity; reabsorption corrections were negligible in the dilute solutions ($c < 10^{-5}$ M) employed.

Time-correlated single-photon counting measurements of nanosecond excited-state fluorescence lifetimes were measured with a Coherent picosecond laser excitation source and a home-built detection and data-processing system that has been described previously.[29] Typical measurements involved the excitation of dilute solutions of the corroles ($c < 10^{-5}$ M) within their strong Soret ($S_2 \leftarrow S_0$) absorption bands near 400 nm and observing a narrow bandwidth of dispersed fluorescence from the vibrationally relaxed lower-energy S_1 state that is produced in high quantum yield[17] via S_2-S_1 internal conversion. Typically,

(29) Kowalska, D.; Steer, R. P. *J. Photochem. Photobiol. A* **2008**, *195*, 223.

$>10^4$ counts were accumulated in the maximum channel, and deconvolution of the measured fluorescence profile from the instrument response function (ca. 100 ps width) was straightforward, yielding reduced χ^2 values between 1.00 and 1.10 and a random distribution of weighted residuals for both single and double exponential fits.

Time bases were carefully calibrated, and multiple replicate measurements were made to ensure reproducibility. The resulting fluorescence lifetimes reported are averages; those resulting from single exponential fits have a 2σ error of $\pm$ 0.05 ns, whereas double exponential fits produce lifetimes with a slightly larger estimated error.

Acknowledgment. The authors are grateful for the continuing support of this research by the Natural Sciences and Engineering Research Council of Canada. A.M. and Z.G. wish to acknowledge the Binational U.S.−Israel Science foundation. The support of the Canada Foundation for Innovation, the Saskatchewan Structural Sciences Centre, and the assistance of Dr. Sophie Brunet with laser maintenance and training are also gratefully acknowledged.

Supporting Information Available: Additional text giving the set of processes used to construct the kinetic model for the system under consideration. This material is available free of charge via the Internet at http://pubs.acs.org.

IC900056N